4 Results and discussion

This chapter presents the micro-structural, meso-structural and macro-structural results related to peach palm. Microscopic techniques and Digital Image Processing were used to determine micro-structure and fibre measurements, establishing the volume fraction of cellulose fibres in the cross section of peach palm and then to classify them as functionally graded material (FGM). Furthermore, the basic physical properties (moisture and specific gravity) and mechanical properties to tension, flexion and torsion; reporting results the maximum tensile strength (TS), the tensile modulus of elasticity (TMOE), bending modulus of elasticity (BMOE) and modulus of rigidity (MOR) were determined adjusting results with statistical methods to ensure test accuracy.

4.1. Micro-structural description

The microstructure of studied peach palm is presented in Figure 4.1.

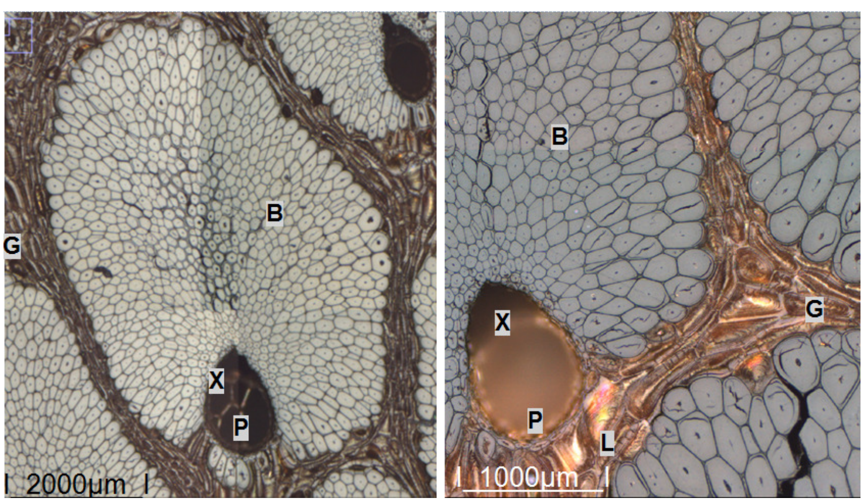

Figure 4.1. Transverse sections depicting developmental changes of stem tissue at chest height for peach palm. 1. Peripheral stem tissue. 2. Central stem tissue. Ground tissue (G) consists of parenchyma cells with lacunae (L) forming in the central ground tissue. Vascular bundles consist of the xylem (X), phloem (P), and bundle sheath (B).

This micro-structure is consistent with the observations of Ritch's study (1987) where the general anatomy within individual stems of the palms: *Iriartea Gigantea* and *Welfia georgii*, have shown similarities in the anatomy of the *Bactris gasipaes Kunth*. These species have a greater concentration of vascular bundles at the stem periphery and peripheral bundles have more extensive fibre sheaths than do central bundles. Peripheral vascular bundles from near the crown are narrower than bundles near the stem base. Leaf and inflorescence traces are more abundant near the crown. Vascular bundle concentration also increases near the crown. For these species, central parenchyma cells are larger than peripheral parenchyma cells. Parenchyma cells size decreases with height position for all species.

4.2.
Meso-structural description

With the aim to obtain and improve the image acquisition method, initially, an image of the same specimens was captured by using two different tools: one image was taken with an optical microscope while the other was obtained using a conventional scanner. After analyzing the obtained imagines, it was clear that both methods were equally efficient. Both allow fibre and matrix segmentation (Figure 4.2).

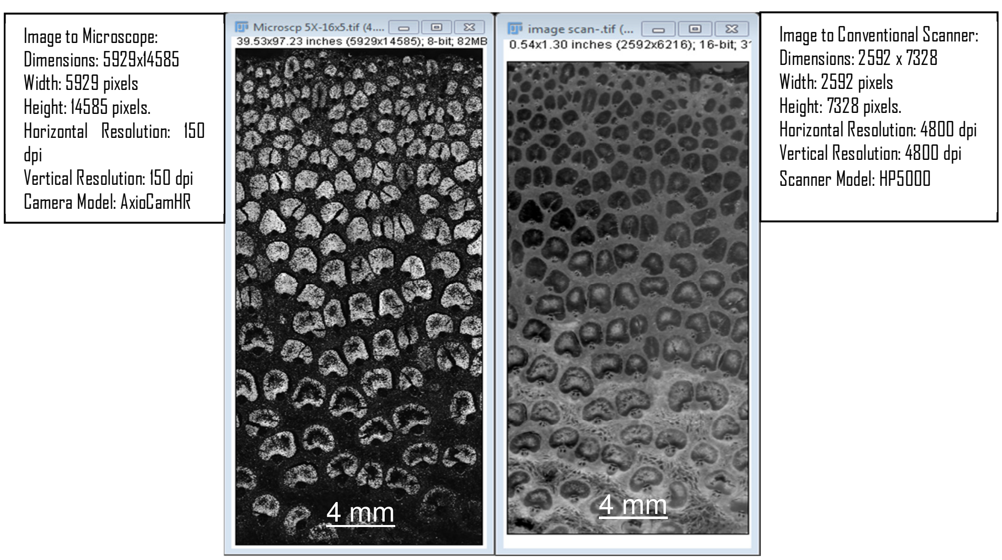

Figure 4.2. Image obtained by: (a) Optical Microscope (b) Conventional Scanner.

Once cut and polished specimens were acquired, images were digitalized using a conventional scanner. Subsequently the pre-processing, segmentation, post -processing and extraction of attributes using the ImageJ software were performed.

The pre-processing stage started with the correction of variations in contrast, which appears as a darker shade in the middle of the image. These variations could be caused by specimen’s preparation or obtention of the image scanner. Such problems not do allow fibre segmentation. The solution was to use a background correction method which produced a highly blurred image, and then a low pass filter was applied to produce an image with a non-uniform background. This image is then subtracted from the original and led to a corrected image which is also shown in Figure 4.3.

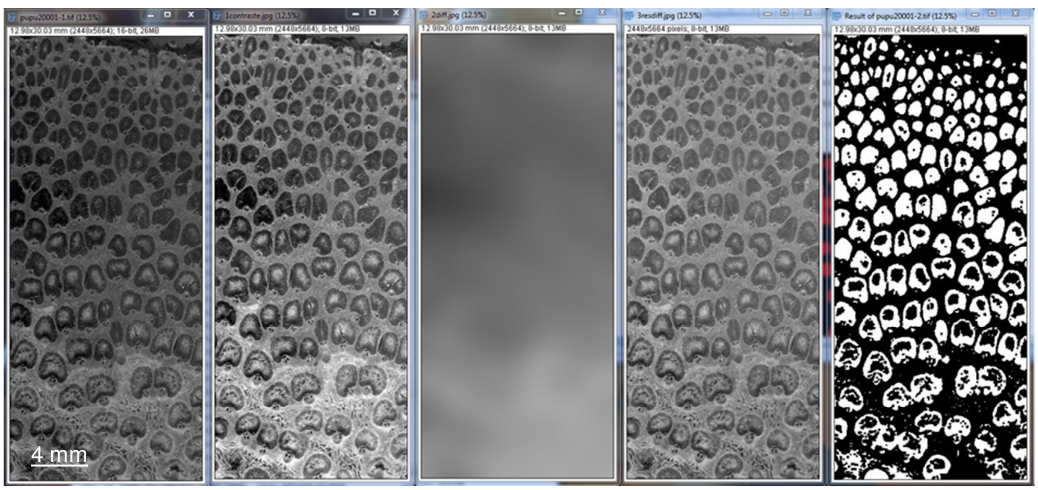

Figure 4.3. Background correction – Low pass filter.

After correcting variations of contrast and converting images to binary (8-bit), only black and white tones were obtained. This was proceeded with an image segmentation. Initially, digital processing tools were applied (remove outlines, and fill holes) in order to achieve a correct color separation using threshold tools. A threshold histogram is shown in Figure 4.4. Further processing was performed using the ImageJ analysis tools creating regions that were initially considered as regions of interest in the segmentation process, as a single attribute extracting the fiber volume fraction of each slice of the original image. The final image with the "attribute extraction" is shown in Figure 4.5

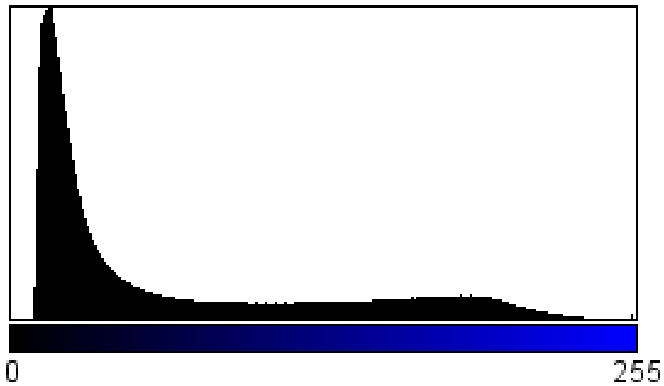

Figure 4.4. Histogram for Threshold tools.

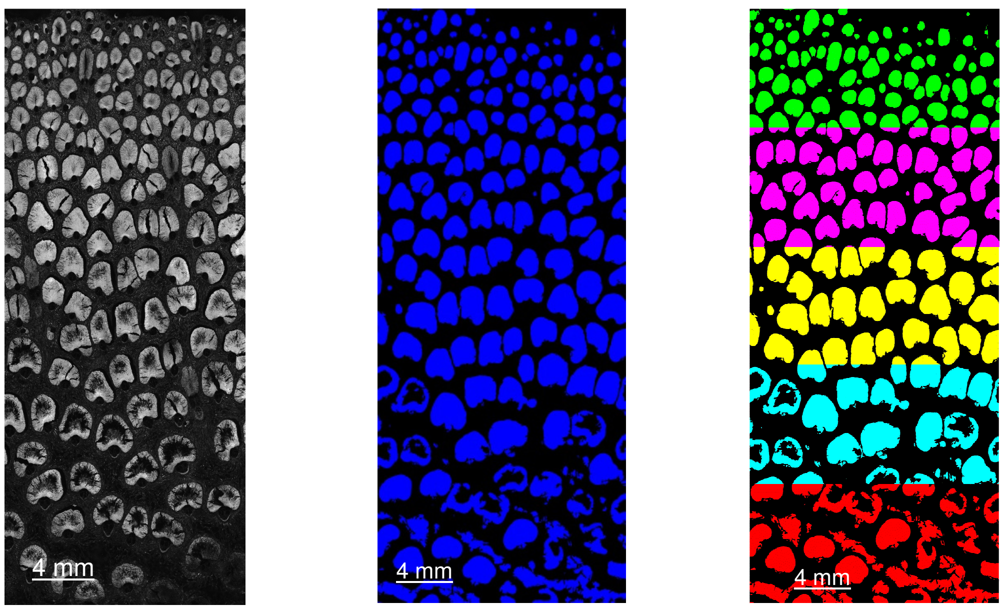

Figure 4.5. Segmentation image for division and calculating the area fiber and matrix.

4.2.1. Fiber volume fraction (V_f) measurements

Each specimen corresponding to each peach palm selected for this study, of 6 and 20 years of age, evidenced a variation of the volume fraction of the fibres.

Through mathematical analysis of the data obtained, polynomial regression curves, two equations were written corresponding to each specimen, in order to apply the rule of mixtures to determine that peach palm is a composite functionally graded material (Figure 4.6).

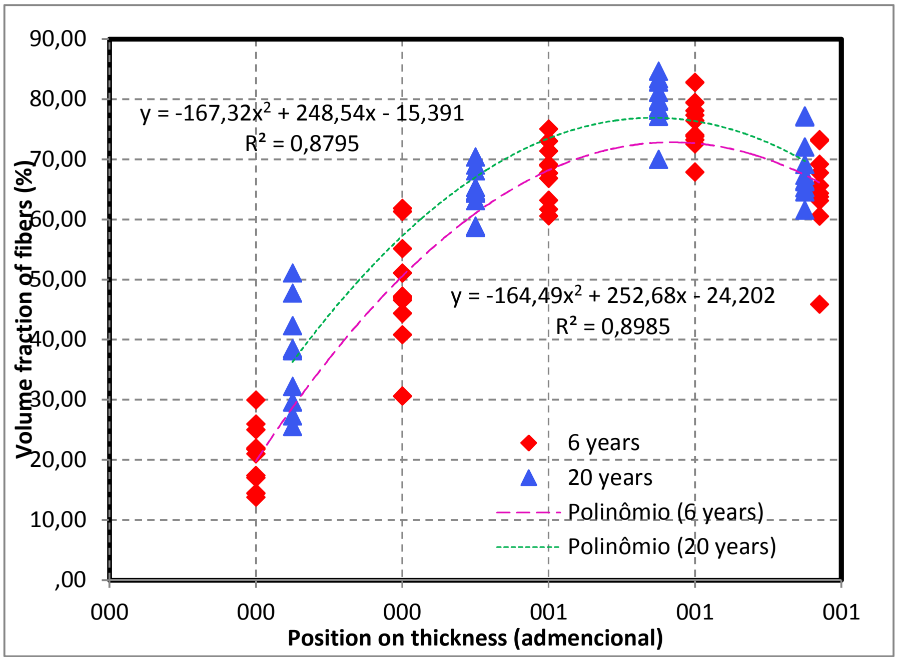

Figure 4.6. Polynomial regression curves.

The variations of fibre for each specimen (6 and 20 years old) are represented by eq. (18) and eq. (19), respectively.

$$V_f(x) = -196{,}11x^2 + 217{,}06x + 15{,}578 \quad (18)$$

$R^2 = 0{,}8649$ for 20 years

$$V_f(x) = -211{,}81\,x^2 + 192{,}05x + 38{,}584 \quad (19)$$

$R^2 = 0{,}8586$ for 6 years

Compared to the variation curve of fibres obtained by Ghavami *et al.*, 2003 in a similar study for bamboo – *Dendrocalamus giganteus* when (eq. (20)),

$$V_f(x) = -8{,}57\,x^2 + 32{,}94x + 28{,}93 \quad (20)$$

Bamboo - *Dendrocalamus giganteus* (DG). The distribution of the fibres along the thickness of the top Section of DG presents a second order equation. The peach palm, in comparison, presents a quadratic equation for the distribution of the fibres along the thickness of the cross-section with a lower concentration of fibres at the external part.

4.2.2. Representative volume element (RVE)

An image analysis of the peach palm section reveals an average of 15 and 60 % with respect to the thickness for peach palms aged more than 12 years.. This region is shown in Figure 4.7 and called "representative volume element (RVE) or unit cell" which is used for mechanical tests.

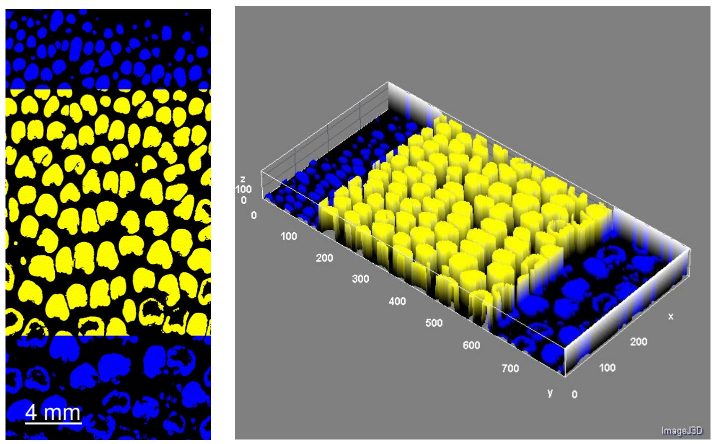

Figure 4.7. Peach Palm representative volume element (RVE) or unit cell.

Additionally, results presented by West (2011) and Ritch (1987) about the longitudinal section of palms stem, showed a high density of fibres at the peripheral area or edges, while specimens tested in this study for Peach Palm showed a lower density of fibres in that same area and different density for ages (Figure 4.8).

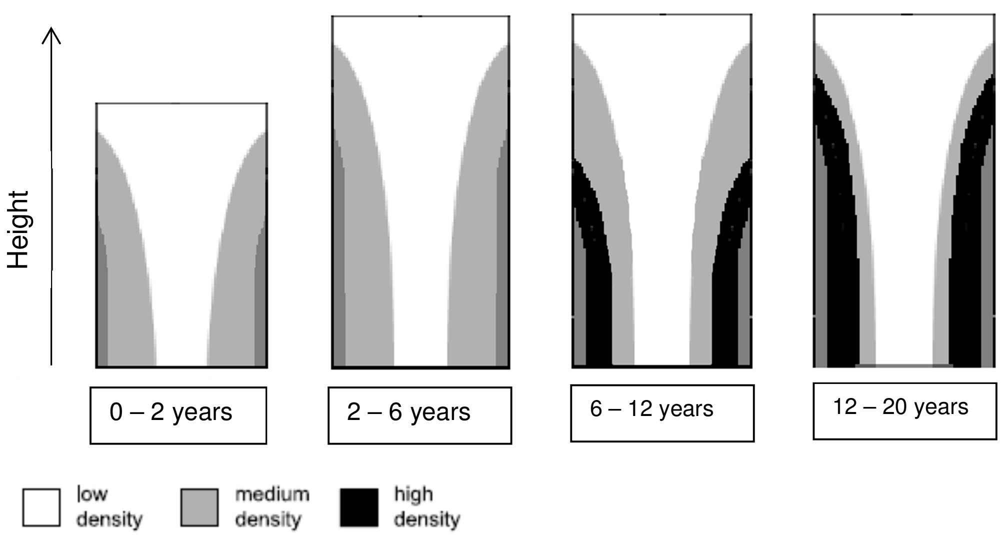

Figure 4.8. Longitudinal section of the peach palms stem. According to fibre density.

4.3. Macro-structural description

4.3.1. Direct Moisture Content

Applying the eq. (21),

$$MC, \% = \frac{A-B}{B} X\ 100 \quad (21)$$

Where:

A = original mass, g,

B = oven-dry mass, g, and

MC is the percentage of water in the specimen and related to the dry mass of the specimen. The results from Figure 4.9 and Table 4.1. are for two ages of peach palm specimens

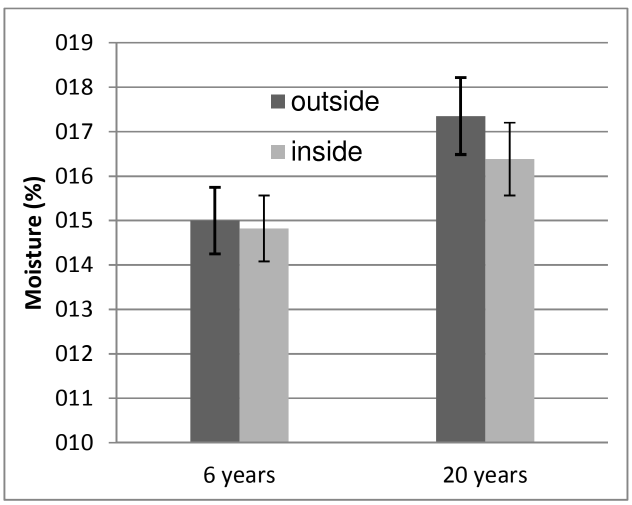

Figure 4.9. Direct Moisture Content for 2 ages of peach palm.

Table 4.1. Peach Palm Direct Moisture Content.

	Number of Specimens	Moisture Content MC (%)			Standard deviation
		Inside	Outside (RVE)	Mean	
Sample 6 years	10	14,82	15,00	14,91	0,393
Sample 20 years	16	16,38	17,35	16,87	0,327

4.3.2.
Specific Gravity (SG)

Operations were carried out immediately after drying, weighing, calculating the mass of specimens with an accuracy of 0.01 g, applying the eq. (22),

$$S = Km_o/V = (Km_o)/(Ltw) \qquad (22)$$

Where:

m_o= final (oven-dry) mass of specimen

V = $L\ t\ w$, volume of specimen as measured at the time of test;

L = length of specimen;

t = thickness of specimen;

w = width of specimen; and

K = constant whose value is determined by the units used to measure mass and volume:

K = 1.00 when mass is in g and volume is in cm^3

Specific gravity (SG) is calculated based on oven-dry mass and volume and is the percentage of water in the specimen related to the dry mass of the specimen.

The results of SG shown in Figure 4.10 and Table 4.2. are for two ages of peach palm specimens

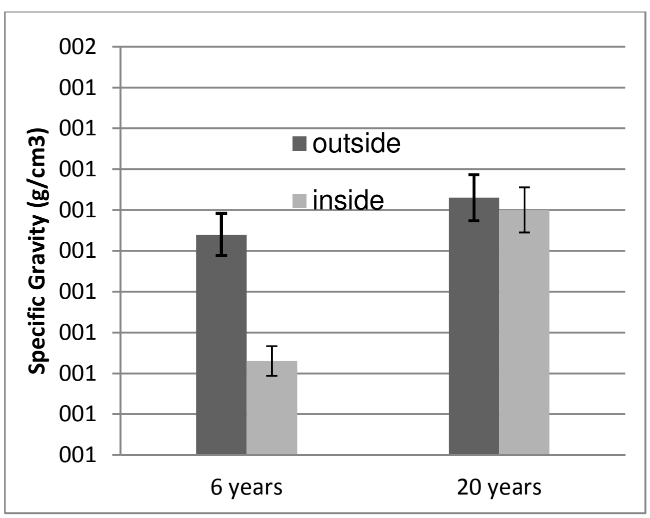

Figure 4.10. Specific gravity (SG) for 2 ages of peach palm.

Table 4.2. Peach Palm Specific gravity (SG)

	Number of Specimens	Specific Gravity (gr/cm3)			Standard deviation
		Inside	Outside	Mean	
Specimen 6 years	10	0,73	1,04	0,88	0,09
Specimen 20 years	12	1,10	1,13	1,12	0,01

According to Acha (2011) for bamboo- *Dendrocalamus Gigantescus*, specific gravity (SG) varies between 0.4 to 0.8 approximately and its moisture content (MC) varies from 155% to 70% from the innermost layers to the peripheral layers in some species, finding that the peach palm has higher density and lower moisture content when compared to bamboo – *Dendrocalamus Gigantescus*.

4.3.3. Tensile Properties

4.3.4. Tensile Strength (TS)

The tensile strength was determined by performing test bodies according to ISO 314 and ASTM 3039, for two ages of peach palm. The specimens were manufactured using the representative volume element (RVE) and tested on servo hydraulic - universal machine INSTRON (Figure 4.11).

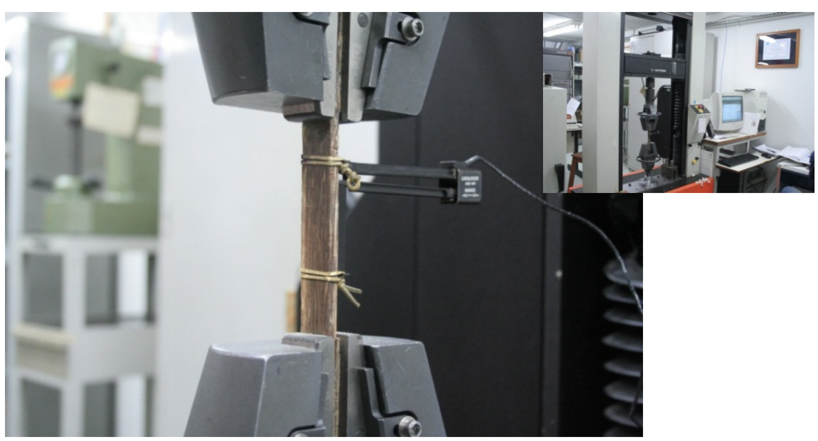

Figure 4.11. Servo hydraulic - universal machine INSTRON for tension test.

Figure 4.12 shows specimens results of ISO 314, and Figure 4.13 for ASTM D3039, once testing determined that the results obtained from specimen’s manufactured with ISO314 standard guidelines did not present reliable results, given that the material fracture occurred in reduction or gripping areas. The specimen’s manufactured to the ASTM guidelines presented satisfactory results for classifying the type of fracture according to this standard.

Figure 4.12. Final Result Specimens for ISO314 tension test.

Figure 4.13. Final Result Specimens for ASTM3039D tension test.

4.3.5.
Tensile Modulus of elasticity (TMOE)

Figure 4.14 shows the stress - strain curve, with the aim of determining the tensile modulus of elasticity (TMOE) for different ages of the peach palm specimens. This module was automatically found by the software supplied with the universal testing machine Instron.

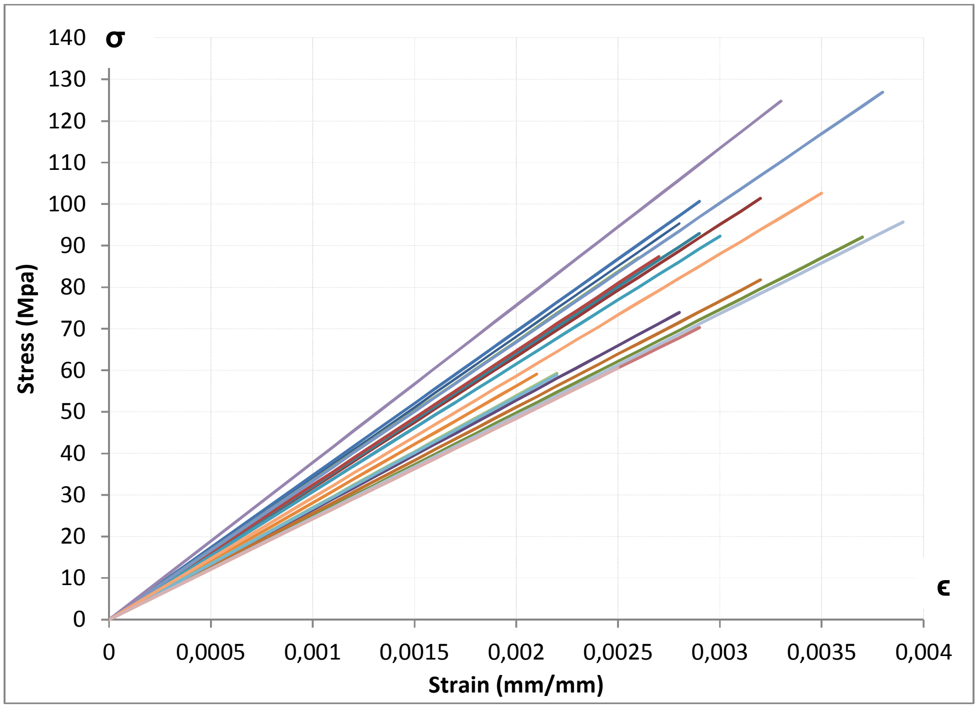

Figure 4.14. Peach Palm stress vs. strain curves.

The sampling method for the tensile strength and modulus of elasticity were validated against the probability distribution mostly used (Figure 4.15 and 4.16). Obtained results showed that combining parametric and non-parametric probability methods, allows to identify the most appropriate probability distribution, which makes possible a more accurate estimation of the parameters, mainly the characteristic value that it is critically significant in the area of natural composite materials. The results obtained are presented in Tables 4.3 to 4.7.

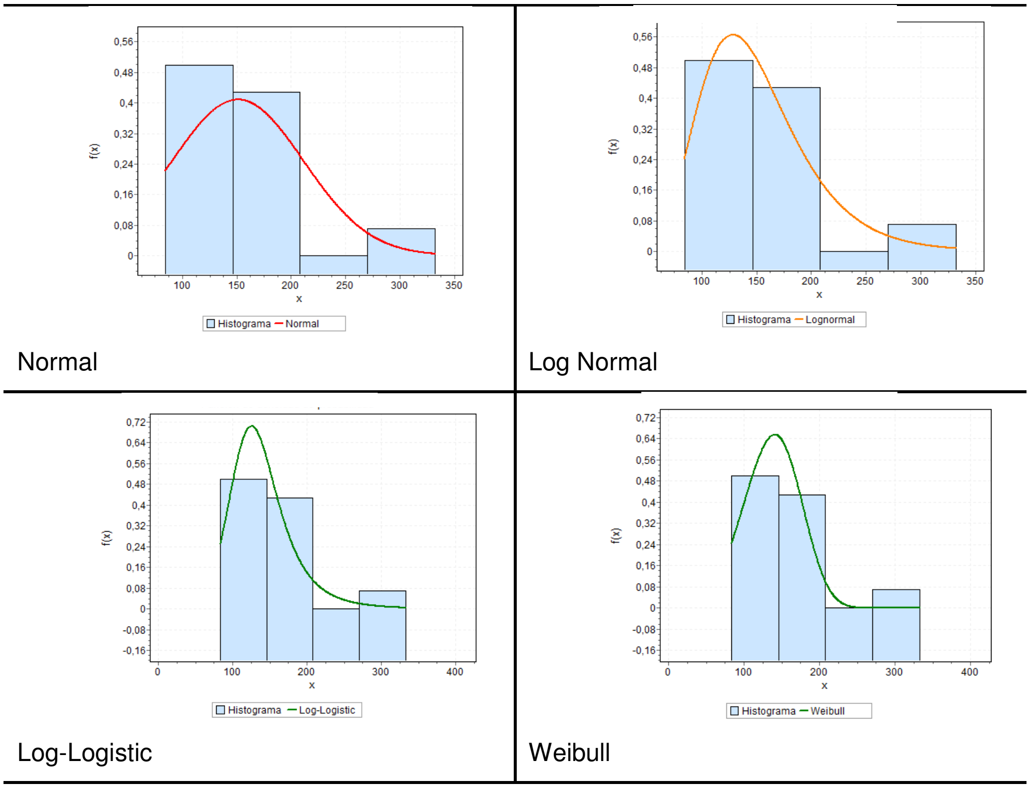

Figure 4.15. Probability graphs most used for tensile strength.

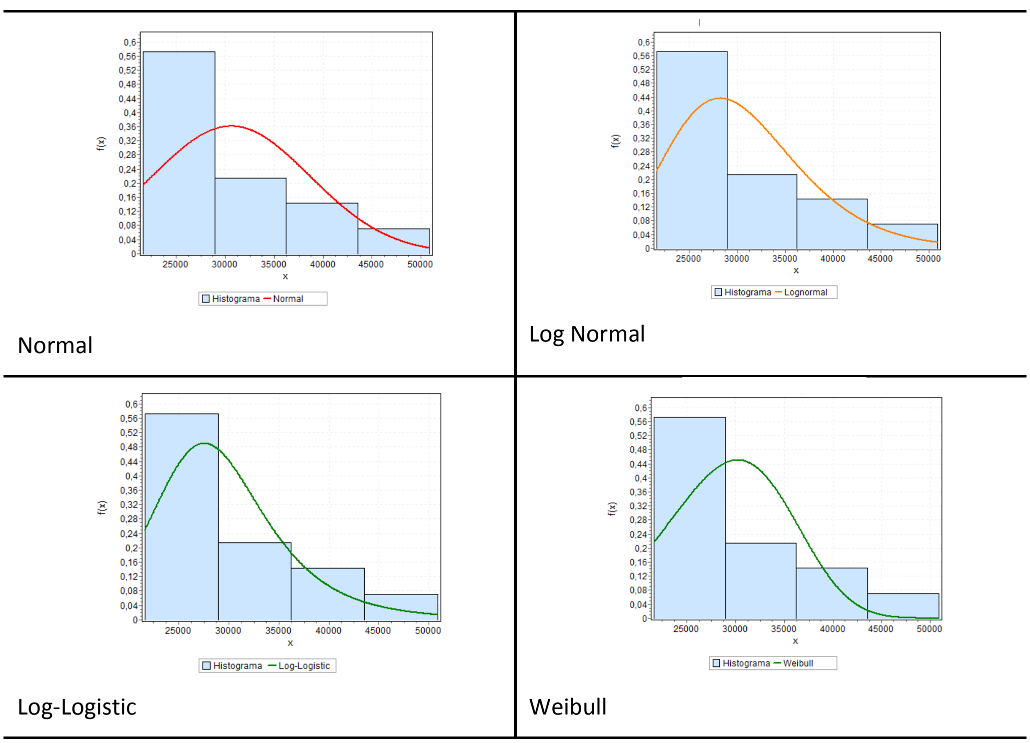

Figure 4.16. Probability graphs most used for modulus of elasticity.

Table 4.3. Probability distribution for Maximum Tensile Stress (age: 6 years).

Maximum Tensile stress (6 years)				
Probability distribution	Normal	Log-Normal	Log-Logistic	Weibull
Number Specimens	20	20	20	20
Mean (MPa)	83,44	83,44	83,44	83,44
Standard Deviation	13,71	0,15	1,33	0,95
PERCENTIL 5	56,46	56,46	77,51	77,51
Characteristic Value (MPa)	50,86	56,40	76,76	76,98

Table 4.4. Probability distribution for Maximum Tensile Stress. (age: 20 years)

Maximum Tensile stress (20 years)				
Probability distribution	Normal	Log-Normal	Log- Logistic	Weibull
Number Specimens	20	20	20	20
Mean (MPa)	147,91	147,91	147,91	147,91
Standard Deviation	60,68	0,32	5,88	4,18
PERCENTIL 5	105,03	105,03	105,03	105,03
Characteristic Value (MPa)	79,02	104,89	102,51	103,23

Table 4.5. Probability distribution for Elastic Modulus (age: 6 years).

Young's Modulus (6 Years)				
Probability distribution	Normal	Log-Normal	Log-Logistic	Weibull
Number Sp.	20	20	20	20
Mean (MPa)	29206,1	29206,1	29206,1	29206,1
Standard Deviation	4326,0	3,2	1,7	4,3
PERCENTIL 5	24158,9	24158,9	25145,1	25145,1
Characteristic Value (MPa)	21998,5	24157,3	25144,3	25142,9

Table 4.6. Probability distribution for Elastic Modulus (age: 20 years).

Young's Modulus (20 Years)				
Probability distribution	Normal	Log-Normal	Log-Logistic	Weibull
Number Sp.	20	20	20	20
Mean (MPa)	30726,2	30726,2	30726,2	30726,2
Standard Deviation	7588,5	5,2	2,9	7,5
PERCENTIL 5	22969,4	22969,4	22969,4	22969,4
Characteristic Value (MPa)	19544,5	22967,1	22968,1	22966,0

Table 4.7. Finally results.

	Number of Specimens	**Maximum Tensile stress** MPa	**Young's Modulus** MPa	**Standard deviation**	**Probability distribution**	**Moisture Content MC** (%)
Sample 6 years	20	76,98	25142,9	4,3	Weibull	14,91
Sample 20 years	20	103,23	22966,0	7,5	Weibull	16,87

4.3.6. Tensile Failure

According to the way of failure occurring in tensile test, typical modes of error codes tensile test were compared to those presented in ASTM D3039, concluding that peach palm tensile failure is similar to the code figure “Long Splitting Gage Middle (SGM)” in typical modes of the error codes ASTM D3039 (Figure 4.17).

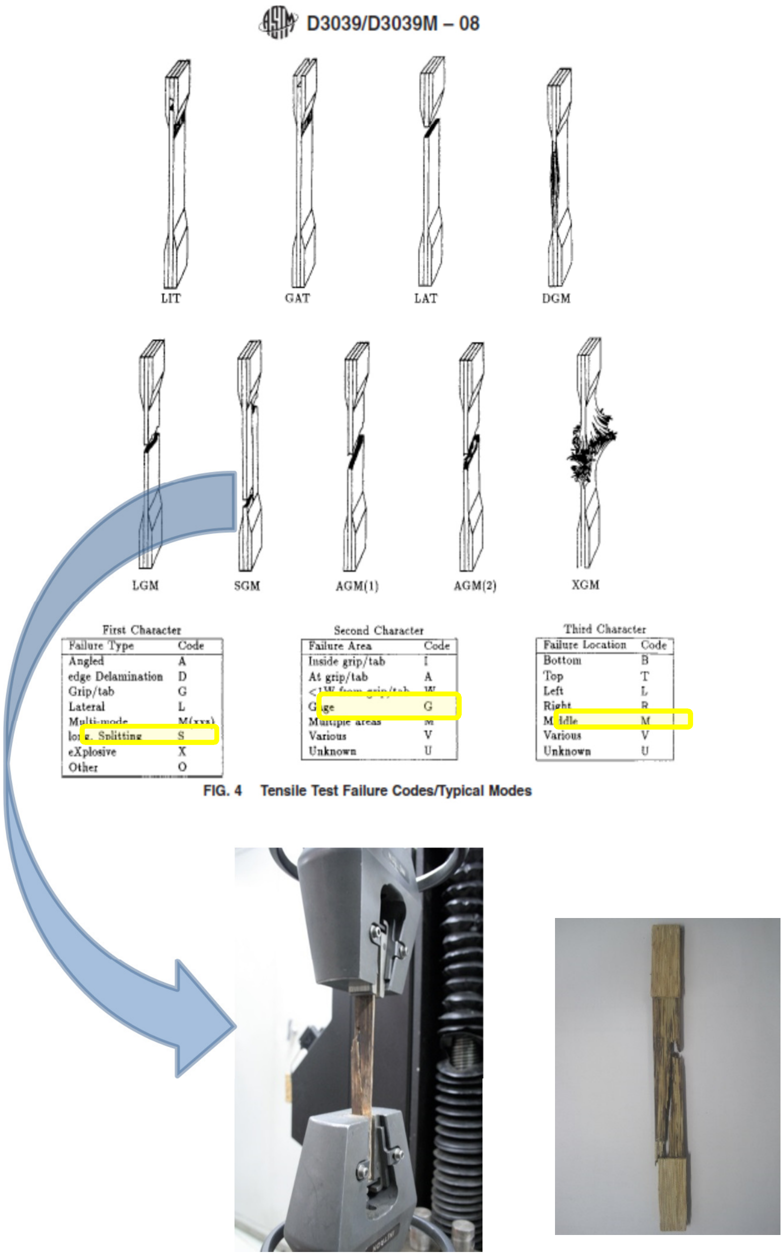

Figure 4.17. Peach Palm error code to tensile test.

4.3.7.
Bending and torsion properties

Using representative volume element (RVE) in cross section obtained by digital processing, specimens were developed for bending and torsion tests. These tests were conducted in the laboratory testing machine for bio-materials, "Universidad del Valle - Colombia " (Figure 4.18).

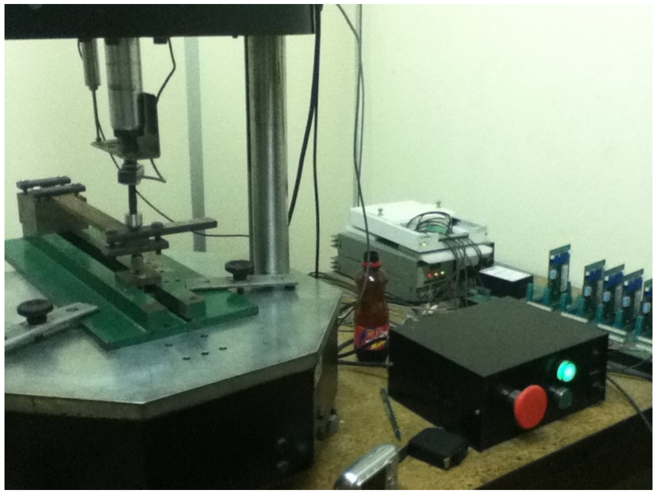

Figure 4.18. Test Machine for Bending and Torsion. Bio-materials Laboratory – Universidad del Valle – Cali, Colombia.

4.3.8. Bending modulus of elasticity (BMOE)

For the bending test (Figure 4.19), the expression for calculating the deflection "d" overhang occurs at the free end of which the value is given by eq. (23). Results solving bending modulus of elasticity (BMOE) for elastic-linear material (n=1) are shown in Table 4.8.

$$\delta = \frac{L^{n+2}}{n+2}\left(\frac{F}{EI_n}\right)^n \rightarrow n = 1 \rightarrow \delta = \frac{FL^3}{3EI_1}$$

$$E = \frac{FL^3}{3\delta I} \qquad (23)$$

Where:

E = Elasticity Modulus. (MPa)

F = Force. (N)

L = Long. (m)

δ = Deflection. (m)

I = Inertia. (m^4).

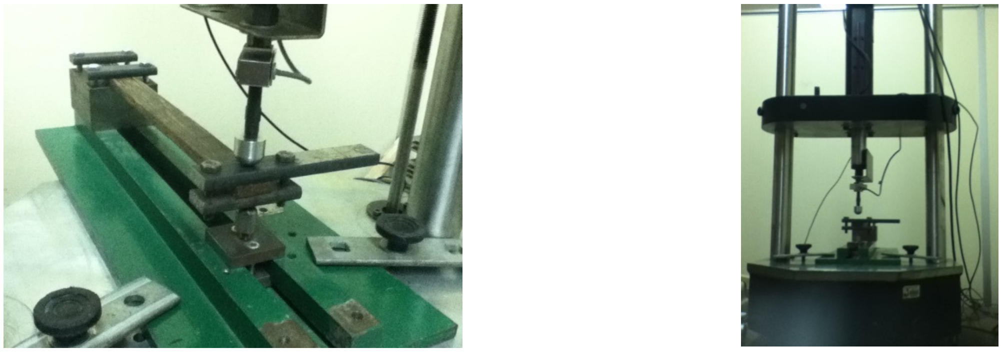

Figure 4.19. Cantilever test where the arrow d is obtained, along with the value of the applied load.

Table 4.8. Results of flexural elasticity modulus in cantilever Test.

	Number of Specimens	bending modulus of elasticity (BMOE) GPa	Standard deviation
Sample 6 years	14	**21,444**	**1,15**
Sample 20 years	14	**24,703**	**1,90**

4.3.9. Shear Modulus or Modulus of Rigidity (MOR)

The pure torsion test consisted of applying load to the specimen cantilever with one end restrained in all directions. Then the torsional load was applied at the free end through a metallic bar as shown in Figure 4.20.

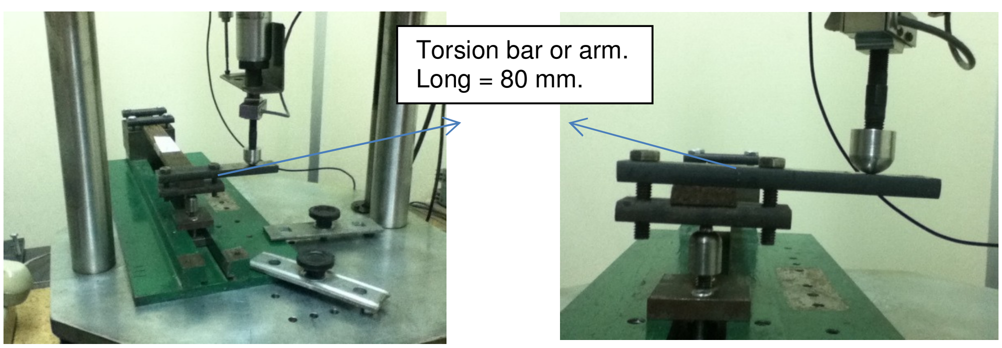

Figure 4.20. Torsion test.

With the data supplied by the torsion test, the shear modulus or modulus of rigidity was calculated from standard mechanical formulae for beams (eq. (24)) of rectangular cross section (Timoshenko 1956). Results are presented in Table 4.9

$$G = \frac{M_t}{\theta \beta a b^3} = \frac{T^2 P l}{\beta a b^3} \quad (24)$$

Where:

G	= Modulus of Rigidity. (Mpa)
Mt	= Torsion Moment. = $T \cdot P$
P	= Force. (N)
θ	= torsion angle = $\frac{\delta}{Tl}$
δ	= Deflection (by torsion) (m)
T	= Arm long. (torsion bar) (m)
l	= specimen long. (m)
β	= Coefficient beta depending on the ratio between the width (a) and thickness (b) Table 3.3
a	= Width (m)
b	= Thickness (m)

Table 4.9. Results the shear modulus or modulus of rigidity in Torsion Test.

	Number of Specimens	Shear modulus MPa	Standard deviation
Specimen 6 years	14	**533,32**	**200,36**
Specimen 20 years	14	**752,63**	**196,87**

Table 4.10 shown comparative results with different species of bamboo and peach palms.

Table 4.10. Modulus of rigidity for bamboo and Palms.

	Mean values for modulus of rigidity.		
	Bamboo		Palms
	Guadua Angustifolia	*Phyllostachys Pubescens*	*Bactris Gasipaes* (present study)
Martinez, D	712 MPa		752,63 MPa
Garcia, J	581 MPa		
Torres, L.		665 MPa	

Table 4.11 shown optimal age and characteristics for use as structural members in the laminated shape.

Table 4.11. Optimal age for structural use.

Age	Moisture Content MC (%)	Specific Gravity (SG)	Maximum Tensile stress	Young's Modulus (TMOE)	Bending modulus of elasticity (BMOE)	Modulus of Rigidity (MOR)
		gr/cm^3	MPa	GPa	GPa	MPa
20 years	16,87%	1,12	103,23	22,96	24,70	752,63